

Measurement-Based Quantum Metropolis Algorithm

Jonathan E. Moussa¹

¹*Molecular Sciences Software Institute, Virginia Tech, Blacksburg, Virginia 24060, USA**

We construct a measurement-based quantum extension of a rejection-free classical Metropolis algorithm to sample expectation values of observables for quantum Hamiltonians at thermal equilibrium. Observable measurements are incorporated into a thermalizing quantum Markov chain to avoid disturbing it. Our use of Hamiltonian simulation for Gaussian-filtered quantum phase estimation sets a thermalization timescale inversely proportional to temperature. The rejection-free classical algorithm artificially mimics a quantum limitation of indirect access to stationary states of the Hamiltonian.

Originating from the classical Metropolis algorithm [1], classical Markov chain Monte Carlo (MCMC) algorithms are now the dominant paradigm for simulations of classical many-body systems in equilibrium [2]. Although classical MCMC algorithms can also simulate quantum many-body systems, they often must add a bias to avoid an exponential growth of sample variance with system size [3]. It is widely believed [4] that universal, efficient, unbiased sampling of quantum many-body systems requires quantum algorithms run on quantum computers, and an obvious possibility is a quantum extension of a classical MCMC algorithm.

The difficulty of quantum extensions are limited access to energies E_a and stationary states $|\psi_a\rangle$ of a Hamiltonian

$$H = \sum_a E_a |\psi_a\rangle\langle\psi_a| \quad (1)$$

when sampling its thermal state, $\rho_T = e^{-H/T} / \text{tr}(e^{-H/T})$, at a temperature T . In the classical case, we can compute E_a efficiently given a . In the quantum case, our access to H is typically limited to quantum operations like $U(t) = e^{-iHt}$, controlled- $U(t)$, and other unitary functions of H . We may also have access to H as a sum of noncommuting operators with adjustable coefficients. H is then accessible enough to define quantum Markov chains that equilibrate to ρ_T [5–8], including two quantum forms of the Metropolis algorithm [6, 7]. Unfortunately, observable measurements disturb the quantum Markov chain, and each step of the chain requires long-time Hamiltonian simulation to equilibrate accurately to ρ_T , either by slowly driving weak system-bath couplings or precisely resolving E_a in quantum phase estimation.

There are quantum algorithms that prepare ρ_T without a Markov chain, but they have even larger drawbacks beyond the known set of easy instances [9]. The available unbiased algorithms [10–14] all have effective costs per sample that increase exponentially with system size at low temperature. There is a growing interest in algorithms suitable to run on upcoming quantum hardware, based on thermofield double states [15–17] and imaginary time evolutions [18, 19], but

they are not capable of general, unbiased sampling.

In this Letter, we present a measurement-based quantum Metropolis algorithm that surpasses prior proposals [6, 7]. Thermalization is driven by measurements of a local basis $\langle\phi_a|$ to sample the expectation value of an observable

$$B = \sum_a \beta_a |\phi_a\rangle\langle\phi_a| \otimes I \quad (2)$$

repeatedly during long, thermalizing Markov chains rather than only at the end of short Markov chains. An unknown mixing time then causes an unknown autocorrelation time for observable measurements rather than an unknown bias. Quantum phase estimation is filtered using a Gaussian for accurate quantum detailed balance that costs $\mathcal{O}(1/T)$ time in Hamiltonian simulations, as efficient as the hypothetical imaginary-time evolution, $\rho_T \propto U(-i/T)$. Consequently, its energy resolution is too low to implement the rejection steps of previous algorithms accurately. We are not able to fix the rejection step and instead base a quantum algorithm on a rejection-free classical algorithm. Our algorithm has the same caveat as every MCMC algorithm, that its mixing times are likely to be very long when thermal states encode unknown solutions to hard computational problems [20].

The motivation of our rejection-free classical Metropolis algorithm is to thermalize with a limited set of ingredients that mimic quantum limitations. Specifically, we can only transform between states $|\psi_b\rangle\langle\psi_b|$ and $|\psi_a\rangle\langle\psi_a|$ according to a symmetric conditional probability distribution $P(a|b)$ and cannot return to $|\psi_b\rangle\langle\psi_b|$ deterministically. It remains possible to thermalize using our algorithm in Fig. 1 that is inspired by a delayed-rejection Metropolis algorithm [21]. Fig. 1 defines a Markov chain decomposed into branches,

$$P_M(a|b) = \sum_{n=0}^{\infty} P_M(n, a|b), \quad (3)$$

```

1:  $a_0 \leftarrow \text{input}$ 
2:  $n \leftarrow -1$ 
3:  $S_0^0 \leftarrow 0$ 
4: repeat ▷ loop over branches
5:    $n \leftarrow n + 1$ 
6:    $a_{n+1} \sim P(a_{n+1}|a_n)$  ▷  $P(a|b) = P(b|a)$  is required
7:    $u \sim \mathcal{U}(0, 1)$  ▷ uniform distribution over  $[0, 1]$ 
8:    $S_{n+1}^{n+1} \leftarrow 0$ 
9:   for  $m \leftarrow n, \dots, 1$  do
10:     $S_{m-1}^n \leftarrow S_{m-1}^{n-1} + s(E_{a_n} - E_{a_{m-1}} + TS_m^n - TS_{m-1}^{n-1})$ 
11:     $S_{n+1}^m \leftarrow S_{n+1}^{m+1} + s(E_{a_m} - E_{a_{n+1}} + TS_m^n - TS_{n+1}^{m+1})$ 
12:  end for ▷  $s(\omega) \equiv -\ln(1 - f(\omega))$ ,  $f$  satisfies Eq. (5)
13: until  $u \leq f(E_{a_{n+1}} - E_{a_0} + TS_{n+1}^1 - TS_0^n)$ 
14: output  $\leftarrow a_{n+1}$ 

```

FIG. 1. Rejection-free classical Metropolis algorithm.

where each sequential branch has the form

$$\begin{aligned}
P_M(n, a_{n+1}|a_0) &= \sum_{a_1, \dots, a_n} P_n \dots P_0 f_n e^{-S_0^n}, \\
P_n &\equiv P(a_{n+1}|a_n), \\
f_n &\equiv f(E_{a_{n+1}} - E_{a_0} + TS_{n+1}^1 - TS_0^n), \\
S_n^m &\equiv -\ln p_{|m-n|}(E_{a_m}, \dots, E_{a_n}), \quad (4)
\end{aligned}$$

based on an acceptance function $f(\omega)$ and probabilities p_n of delaying acceptance n times after a specific sequence of energies. If the acceptance function satisfies

$$0 \leq f(\omega) \leq 1 \quad \text{and} \quad f(\omega) = f(-\omega)e^{-\omega/T}, \quad (5)$$

then each branch satisfies classical detailed balance,

$$P_M(n, a|b)e^{-E_b/T} = P_M(n, b|a)e^{-E_a/T}. \quad (6)$$

There are numerical problems with the standard choice of $f(\omega) = \min\{1, e^{-\omega/T}\}$ because of infinities in S_n^m that can be fixed with $f(\omega) = (1 - \delta) \min\{1, e^{-\omega/T}\}$ for $\delta \ll 1$.

Our rejection-free classical Metropolis algorithm is only useful for $P(a|b)$ that explore a limited configuration space to enable indirect rejection by rapidly returning to an input state. Otherwise, it can be difficult to return to a low-energy state for large configuration spaces with a small population of low-energy states. To thermalize effectively and explore the entire configuration space, we should alternate between multiple $P_M(a|b)$ defined by different $P(a|b)$. This usage is comparable to the single-site spin flips that are prescribed in the simplest applications of the Metropolis algorithm to the Ising model. Correspondingly, any quantum extension should alternate between different local measurements that traverse the Hilbert space with intensive excitations.

Thermalizing quantum Markov chains are implemented by repeating a quantum operation \mathcal{Q} . In a transition basis,

$$\mathcal{Q}(\rho) = \sum_{a,b,c,d} \mathcal{Q}_{abcd} |\psi_a\rangle\langle\psi_b| \rho |\psi_c\rangle\langle\psi_d|, \quad (7)$$

```

1:  $\rho \leftarrow \text{input}$ 
2:  $n \leftarrow -1$ 
3:  $S_0^0 \leftarrow 0$ 
4:  $\tilde{S}_0^0 \leftarrow 0$ 
5:  $(\omega_0, \rho) \sim \sqrt{g_\lambda(H - \omega_0)}\rho\sqrt{g_\lambda(H - \omega_0)}$  ▷  $g_\lambda$  from Eq. (10)
6: repeat ▷ loop over branches
7:    $n \leftarrow n + 1$ 
8:    $(d_n, \rho) \sim (\langle\phi_{d_n}| \otimes I)\rho(|\phi_{d_n}\rangle \otimes I)$ 
9:    $c_n \sim P(c_n|d_n)$  ▷  $P(a|b) = P(b|a)$  is required
10:   $\rho \leftarrow |\phi_{c_n}\rangle\langle\phi_{c_n}| \otimes \rho$ 
11:   $(\omega_{n+1}, \rho) \sim \sqrt{g_\lambda(H - \omega_{n+1})}\rho\sqrt{g_\lambda(H - \omega_{n+1})}$ 
12:   $u \sim \mathcal{U}(0, 1)$  ▷ uniform distribution over  $[0, 1]$ 
13:   $S_{n+1}^{n+1} \leftarrow 0$ 
14:   $\tilde{S}_{n+1}^{n+1} \leftarrow 0$ 
15:  for  $m \leftarrow n, \dots, 1$  do
16:     $S_{m-1}^n \leftarrow S_{m-1}^{n-1} + s(\omega_n - \omega_{m-1} + T\tilde{S}_n^m - T\tilde{S}_{m-1}^{n-1} + \frac{1}{2\lambda T})$ 
17:     $\tilde{S}_{m-1}^n \leftarrow \tilde{S}_{m-1}^{n-1} + s(\omega_n - \omega_{m-1} + T\tilde{S}_n^m - T\tilde{S}_{m-1}^{n-1})$ 
18:     $S_{n+1}^m \leftarrow S_{n+1}^{m+1} + s(\omega_m - \omega_{n+1} + T\tilde{S}_m^n - T\tilde{S}_{n+1}^{m+1} + \frac{1}{2\lambda T})$ 
19:     $\tilde{S}_{n+1}^m \leftarrow \tilde{S}_{n+1}^{m+1} + s(\omega_m - \omega_{n+1} + T\tilde{S}_m^n - T\tilde{S}_{n+1}^{m+1})$ 
20:  end for ▷  $s(\omega) \equiv -\ln(1 - f(\omega))$ ,  $f$  satisfies Eq. (5)
21: until  $u \leq f(\omega_{n+1} - \omega_0 + T\tilde{S}_{n+1}^1 - T\tilde{S}_0^n + \frac{1}{2\lambda T})$ 
22:  $\omega_0 \leftarrow \frac{1}{2\lambda T} + \omega_0 e^{-1/(4\lambda T^2)}$ 
23: output  $\leftarrow (\rho, \omega_0, d_0)$ 

```

FIG. 2. Measurement-based quantum Metropolis algorithm. We denote measurement of a POVM X_a on ρ as $(a, \rho) \sim X_a \rho X_a^\dagger$.

the trace preservation of ρ requires that

$$\sum_a \mathcal{Q}_{abca} = \delta_{bc}, \quad (8)$$

and standard quantum detailed balance [22] requires that

$$\mathcal{Q}_{abcd} e^{-E_{bc}/T} = \mathcal{Q}_{badc}^* e^{-E_{ad}/T} \quad (9)$$

for $E_{ab} = (E_a + E_b)/2$. If we contract b and c in Eq. (9) and use Eq. (8) to remove \mathcal{Q}^* , then $\mathcal{Q}(\rho_T) = \rho_T$. Therefore Eqs. (8) and (9) guarantee that ρ_T is stationary for \mathcal{Q} .

Gaussian-filtered quantum phase estimation (GQPE) is a key quantum computational primitive of our algorithm that is inspired by the quantum spectral filtering algorithm [23] and defined by a normalized Gaussian filter,

$$g_\lambda(\omega) = \sqrt{\lambda/\pi} e^{-\lambda\omega^2}. \quad (10)$$

For our purposes, we use GQPE to measure the energy of ρ as the outcome ω of a positive-operator valued measure (POVM) sampled from $\text{tr}(\rho g_\lambda(\omega - H))$ with output state

$$\begin{aligned}
\rho_\lambda(\omega) &\propto \sqrt{g_\lambda(\omega - H)}\rho\sqrt{g_\lambda(\omega - H)} \\
&= \sum_{a,b} g_\lambda(\omega - E_{ab}) \gamma_{ab}^\lambda |\psi_a\rangle\langle\psi_a| \rho |\psi_b\rangle\langle\psi_b|, \quad (11)
\end{aligned}$$

for a dephasing factor $\gamma_{ab} = e^{-(E_a - E_b)^2/4}$. Postselection on ω effectively postselects on E_{ab} with acceptance functions in ω and E_{ab} that are related by Gaussian convolution.

Our quantum extension of the rejection-free algorithm is in Fig. 2. Classical state updates using $P(a|b)$ are replaced with local updates where measurement of $\langle\phi_b|$ conditions preparation of $|\phi_a\rangle$. Local updates interleave global GQPE steps that inform acceptance decisions. As in the classical case, this quantum operation decomposes into branches,

$$\mathcal{Q}^M = \sum_{n=0}^{\infty} \mathcal{Q}^{M(n)}, \quad (12)$$

and each branch represented as in Eq. (7) is

$$\begin{aligned} \mathcal{Q}_{a_{n+1}a_0b_0b_{n+1}}^{M(n)} &= \sum_{\substack{a_1, \dots, a_n \\ b_1, \dots, b_n}} G_{n+1} L_n G_n \cdots L_0 G_0 \bar{f}_n e^{-S_0^n}, \\ G_n &\equiv \gamma_{a_n b_n}^\lambda \int_{-\infty}^{\infty} d\omega_n g_\lambda(\omega_n - E_{a_n b_n}), \\ L_n &\equiv \sum_{c_n, d_n} P(c_n | d_n) \Phi_{a_{n+1} a_n}^{c_n d_n} \Phi_{b_n b_{n+1}}^{d_n c_n}, \\ \bar{f}_n &\equiv f(\omega_{n+1} - \omega_0 + T \bar{S}_{n+1}^1 - T S_0^n + \frac{1}{2\lambda T}), \\ S_n^m &\equiv -\ln p_{|m-n|}(\omega_m, \dots, \omega_n), \\ \bar{S}_n^m &\equiv -\ln p_{|m-n|}(\omega_m + \frac{\delta_{mn}}{2\lambda T}, \dots, \omega_n + \frac{\delta_{nn}}{2\lambda T}), \\ \Phi_{cd}^{ab} &\equiv \langle\psi_c|(|\phi_a\rangle\langle\phi_b| \otimes I)|\psi_d\rangle. \end{aligned} \quad (13)$$

While this form is more complicated than Eq. (4), all of its terms except for $G_{n+1} G_0 \bar{f}_n e^{-S_0^n}$ have a clear symmetry and can be removed from Eq. (9). We can further remove E_{ad} , E_{cd} , and $G_{n+1} G_0$ by shifting ω_0 or ω_{n+1} by $\frac{1}{2\lambda T}$ to recover Eq. (5) with some energy shifts in f and S_n^m . The classical acceptance statistics are recovered in the $\lambda \rightarrow \infty$ limit. We can decrease λ to reduce the cost of each GQPE step, but this also reduces acceptance probabilities and increases the average number of GQPE steps before Fig. 2 halts.

The outputs in Fig. 2 are a quantum state to continue the quantum Markov chain and indirect outcomes for H and B measurements on the input state, which is the thermal state ρ_T once the chain has equilibrated. The effect of Gaussian filtering on the thermal expectation value of H is to cause a linear distortion that is corrected on line 22. GQPE causes energy dephasing before the B measurement, but this does not change ρ_T . Thus we can estimate $\text{tr}(\rho_T H)$ and $\text{tr}(\rho_T B)$ without bias by averaging ω_0 and β_{d_0} respectively from the output of Fig. 2. At equilibrium, each quantum Metropolis step collapses ρ_T with a local measurement of B and then repairs the collapsed ρ_T before returning it as output.

Our implementation of GQPE is shown in Fig. 3. It uses a “centered” quantum Fourier transform (CQFT) between

$$t_j = -t_{\max} \sum_{n=1}^p \frac{(-1)^{j_n}}{2^n} \quad \text{and} \quad \omega_j = -\omega_{\max} \sum_{n=1}^p \frac{(-1)^{j_n}}{2^{p-n+1}}, \quad (14)$$

defined using bitwise values j_n on p ancilla qubits, with its frequency interval bounded by $\omega_{\max} = 2^{p-1}\pi/t_{\max}$. It acts

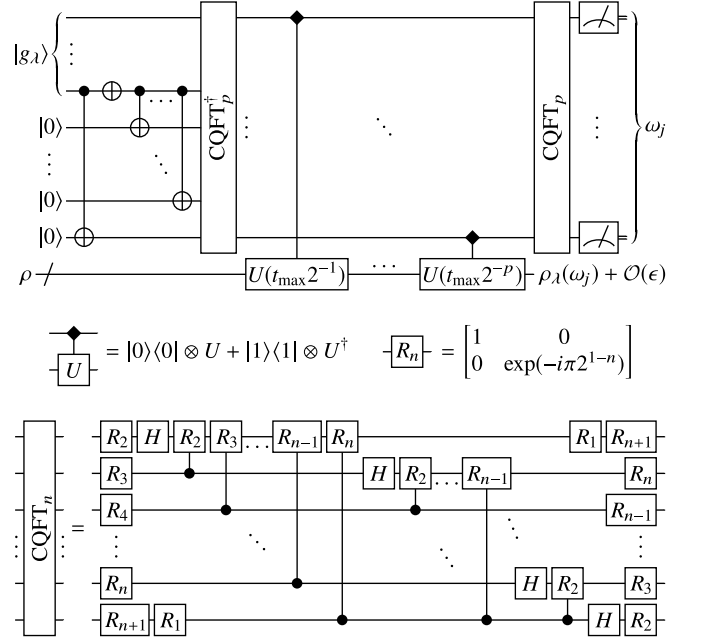


FIG. 3. Gaussian-filtered quantum phase estimation circuit.

as a continuous Fourier transform with controllable errors,

$$\begin{aligned} \epsilon &= \max_{|\omega| \leq E_{\max} + \omega_{\max}} \frac{|g_\lambda(\omega) - \tilde{g}_\lambda(\omega)|}{g_\lambda(0)} \\ &\approx e^{-\min\{t_{\max}^2/(2\lambda), \lambda(2^{p-q}\omega_{\max})^2, \lambda(E_{\max} - \omega_{\max})^2\}}, \\ \tilde{g}_\lambda(\omega) &= \left(\sum_{j=0}^{2^p-1} \sum_{k=0}^{2^q-1} \frac{e^{i(\tilde{\omega}_k - \omega)t_j}}{2^p} \sqrt{g_\lambda(\tilde{\omega}_k)} \right)^2, \end{aligned} \quad (15)$$

for a spectral bound E_{\max} of H , $|E_a| \leq E_{\max}$, that is within the frequency interval, $E_{\max} \leq \omega_{\max}$, and $\sqrt{g_\lambda(\omega)}$ prepared on $q \leq p$ ancilla qubits in a truncated frequency variable,

$$|g_\lambda\rangle \propto \sum_{j=0}^{2^q-1} \sqrt{g_\lambda(\tilde{\omega}_j)} |j\rangle \quad \text{for} \quad \tilde{\omega}_j = \omega_{j+2^{p-1}-2^{q-1}}. \quad (16)$$

The minimized resource requirements for GQPE are

$$\begin{aligned} t_{\max} &\approx \sqrt{2\lambda \ln(1/\epsilon)}, \quad q \approx \lceil \log_2(\ln(1/\epsilon)) \rceil, \\ \text{and } p &\approx \lceil \log_2(E_{\max} t_{\max} + \ln(1/\epsilon)) \rceil. \end{aligned} \quad (17)$$

We can prepare $|g_\lambda\rangle$ in $\mathcal{O}(2^q) = \mathcal{O}(\ln(1/\epsilon))$ gates [24], and more efficient preparation is irrelevant as q is independent of λ and E_{\max} . We assume that errors in $U(t)$ are similarly controlled by ϵ using efficient algorithms [25, 26].

Fig. 3 restricts the POVM outcomes from \mathbb{R} to a grid of frequency values that serve as numerical quadrature points for the integrals in Eq. (13). Eq. (9) remains satisfied by a sum over the frequency grid in Eq. (14) if it obeys

$$t_{\max} = 2\pi\lambda T/z \quad (18)$$

for some integer z , up to a high-frequency truncation error proportional to ϵ . Eqs. (17) and (18) specify λ and t_{\max} up to z , and their resource-minimizing values ($z = 1$) are

$$\lambda = \frac{\ln(1/\epsilon)}{2\pi^2 T^2} \quad \text{and} \quad t_{\max} = \frac{\ln(1/\epsilon)}{\pi T}. \quad (19)$$

This resource optimization does not consider the effects of λ on acceptance statistics, which is difficult to analyze. A crude worst-case analysis wherein acceptance probabilities are $e^{-1/(2\lambda T^2)}$ minimizes the average halting time of Fig. 2 with $\lambda \approx T^{-2}$. This is below the minimal λ for $\epsilon \ll 1$, and a typical-case analysis would prescribe an even smaller λ . Thus, the λ -dependence of acceptance statistics is unlikely to be a determining factor in resource optimization.

Fig. 2 has a well-behaved classical limit similar to Fig. 1 when used with a complete set of commuting observables B_n that commute with H . The quantum state is completely characterized by the measured values of B_n throughout the thermalization process. Finite energy resolution alters the acceptance statistics of the quantum algorithm, but it does not restrict the choice of $f(\omega)$ any more than the classical algorithm. The classical limit is degraded by perturbations of H that do not commute with B_n , which cause measured values of B_n to drift during the quantum Markov chain.

We have established a closest point of approach between classical and quantum many-body simulations where there exists a common MCMC strategy for efficient sampling of classical thermal states on classical computers or quantum thermal states on quantum computers. While these results are irrelevant for upcoming quantum computing hardware that is unlikely to maintain coherence on a thermal mixing timescale, they are impactful to the long-term planning of quantum simulation. Fig. 2 avoids the high cost of precise quantum phase estimation when preparing stationary states [27], and it is capable of preparing ground states of gapped Hamiltonians for temperatures smaller than the energy gap without any need for a large-overlap trial ground state or a large-minimum-gap adiabatic Hamiltonian evolution.

There are many opportunities for further development of quantum MCMC algorithms. Quantum walks can be used instead of $U(t)$ in GQPE to reduce costs [28], but this will complicate satisfying Eq. (9) and measuring H . Replacing local measurements of $\langle \phi_a |$ with global measurements in a basis of approximate stationary states would enable offline reparation and measurement of thermal state samples if the basis has low energy variance. A rejection-free version of cluster updates [29] is possible by temporarily encoding cluster states into small subsystems. Nonsymmetric $P(a|b)$ [30] are possible in a rejection-free algorithm if $P(a|b)$ are used in acceptance decisions to maintain detailed balance. A quantum rejection-free Wang-Landau algorithm [31] is a possibility, but with a minimum accessible temperature set by the GQPE filter width. Finally, quantum effects can be used to accelerate the mixing of Markov chains [7] and the sampling of observable expectation values [32].

This Letter has presented a specific example of a general quantum algorithm design principle. Whenever a quantum algorithm reduces to a classical algorithm in a well-defined classical limit, its development may be decomposable into a more established area of classical algorithm development followed by a quantum extension, which in turn constrains the classical algorithm design. This design strategy may be especially useful in hybrid classical-quantum computation and even more so when it is applied to simulation of hybrid classical-quantum systems. Here, algorithm design would benefit from mimicking the ambiguous classical-quantum boundary of physical systems that depends on the accuracy of their characterization and modeling rather than the clear classical-quantum boundary of digital computers that must be artificially engineered within physical systems.

Norm Tubman was a collaborator on this research. J. E. M. is supported by the National Science Foundation under Grant No. ACI-1547580.

* godotalgorithm@gmail.com

- [1] N. Metropolis, A. W. Rosenbluth, M. N. Rosenbluth, A. H. Teller, and E. Teller, *J. Chem. Phys.* **21**, 1087 (1953).
- [2] D. P. Landau and K. Binder, *A Guide to Monte Carlo Simulations in Statistical Physics*, (Cambridge University Press, Cambridge, 2015).
- [3] M. Troyer and U.-J. Wiese, *Phys. Rev. Lett.* **94**, 170201 (2005).
- [4] R. P. Feynman, *Int. J. Theor. Phys.* **21**, 467 (1982).
- [5] B. M. Terhal and D. P. DiVincenzo, *Phys. Rev. A* **61**, 022301 (2000).
- [6] K. Temme, T. J. Osborne, K. G. Vollbrecht, D. Poulin, and F. Verstraete, *Nature* **471**, 87 (2011).
- [7] M.-H. Yung and A. Aspuru-Guzik, *Proc. Nat. Acad. Sci. USA* **109**, 754 (2012).
- [8] A. Shabani and H. Neven, *Phys. Rev. A* **94**, 052301 (2016).
- [9] F. G. S. L. Brandão and M. J. Kastoryano, *Commun. Math. Phys.* **365**, 1 (2018).
- [10] H. De Raedt, A. H. Hams, K. Michielsen, S. Miyashita, and K. Saito, *Prog. Theor. Phys. Supp.*, **138**, 489 (2000).
- [11] D. Poulin and P. Wocjan, *Phys. Rev. Lett.* **103**, 220502 (2009).
- [12] A. Riera, C. Gogolin, and J. Eisert, *Phys. Rev. Lett.* **108**, 080402 (2012).
- [13] A. N. Chowdhury and R. D. Somma, *Quant. Inf. Comp.* **17**, 41 (2017).
- [14] J. van Apeldoorn, A. Gilyén, S. Gribling, and R. de Wolf, in *Proceedings of the 58th Annual IEEE Symposium on Foundations of Computer Science* (IEEE Computer Society Press, Los Alamitos, CA, 2017), p. 403.
- [15] W. Cottrell, B. Freivogel, D. M. Hofman, and S. F. Lokhande, *arXiv:1811.11528*.
- [16] J. Wu and T. H. Hsieh, *arXiv:1811.11756*.
- [17] J. Martyn and B. Swingle, *arXiv:1812.01015*.
- [18] S. McArdle, T. Jones, S. Endo, Y. Li, S. Benjamin, and X. Yuan, *arXiv:1804.03023*.
- [19] M. Motta, C. Sun, A. T. K. Tan, M. J. O' Rourke, E. Ye, A. J. Minnich, F. G. S. L. Brandão, and G. K.-L. Chan *arXiv:1901.07653*.

- [20] M. Jerrum and A. Sinclair, in *Approximation algorithms for NP-hard problems*, edited by D. S. Hochbaum (PWS Publishing, Boston, 1996), p. 482.
- [21] L. Tierney and A. Mira, *Stat. Med.* **18**, 2507 (1999).
- [22] K. Temme, M. J. Kastoryano, M. B. Ruskai, M. M. Wolf, and F. Verstraete, *J. Math. Phys.* **51**, 122201 (2010).
- [23] F. Fillion-Gourdeau, S. MacLean, and R. Laflamme, *Phys. Rev. A* **95**, 042331 (2017).
- [24] G. H. Low, T. J. Yoder, and I. L. Chuang, *Phys. Rev. A* **89**, 062315 (2014).
- [25] D. W. Berry, A. M. Childs, R. Cleve, R. Kothari, and R. D. Somma, *Forum Math. Sigma* **5**, e8 (2017).
- [26] G. H. Low and I. L. Chuang, *Phys. Rev. Lett.* **118**, 010501 (2017).
- [27] R. Babbush, C. Gidney, D. W. Berry, N. Wiebe, J. McClean, A. Paler, A. Fowler, and H. Neven, *Phys. Rev. X* **8**, 041015 (2018).
- [28] D. Poulin, A. Kitaev, D. S. Steiger, M. B. Hastings, and M. Troyer, *Phys. Rev. Lett.* **121**, 010501 (2018).
- [29] R. H. Swendsen and J.-S. Wang, *Phys. Rev. Lett.* **58**, 86 (1987).
- [30] W. K. Hastings, *Biometrika* **57**, 97 (1970).
- [31] F. Wang and D. P. Landau, *Phys. Rev. Lett.* **86**, 2050 (2001).
- [32] E. Knill, G. Ortiz, and R. D. Somma, *Phys. Rev. A* **75**, 012328 (2007).